BULLETIN OF THE POLISH ACADEMY OF SCIENCES
TECHNICAL SCIENCES, Vol. 59, No. 4, 2011
DOI: 10.2478/v10175-011-0065-3

Three-phase soft-switching inverter with coupled inductors, experimental results

S. KARYŚ*

Power Electronics Department, Kielce University of Technology, 7 1000-lecia P.P. Ave., 25-314 Kielce, Poland

Abstract. This paper presents experimental results of the three-phase soft-switching inverter with coupled inductors that verify the control method influence on efficiency improvement. Different kinds of control methods were tested on the 6 kW experimental inverter. A short discussion on a few design methods of the resonant tank elements was made. Experimental results confirm that the advanced control algorithm and the proposed new design method of the resonant tank elements significantly increase the efficiency of this resonant inverter.

Key words: soft switching, resonant inverter, ZVS inverter.

1. Introduction

Three-phase high efficiency inverters are demandable solution in high power applications, particularly in the electric car drive systems. The soft-switching pole inverters have complex structure and control, only a few of them can obtain higher efficiency than hard switching inverters [1, 2]. The three-phase soft-switching inverter with coupled inductors belongs to them and is shown in Fig. 1. The actual problems related with this kind of inverters are determination how far the advanced control and various design of the resonant tank elements methods influence the efficiency improvement. Introducing high performance DSP microprocessors, CPLD structures and digital control technique, makes it possible to perform complex control algorithms without additional sensors. In spite of the fact that many years since this type of inverters has been elaborated [3, 4], there is no good design procedure for the resonant tank elements selection. Unfortunately, the widely used design method [5] increases the loss in this type of the inverters.

The main transistors T1÷T6 are switched under zero voltage conditions ZVS and the auxiliary transistors Ta1÷Ta6 are switched under zero current conditions ZCS. Therefore this inverter has a very low switching loss. The detailed operation principle and the control algorithm were described in [2]. The control is similar to the auxiliary resonant soft-switched inverter ARCP. On the base of control signals from the primary modulator, the control unit of the inverter with coupled inductors stretches out or cuts down these signals and generates additional one for auxiliary switches. The control signals sequence depends on the phase load current sign i_f. Figure 2 shows the i_L current in one leg of the auxiliary branch and control signals for $i_f > 0$.

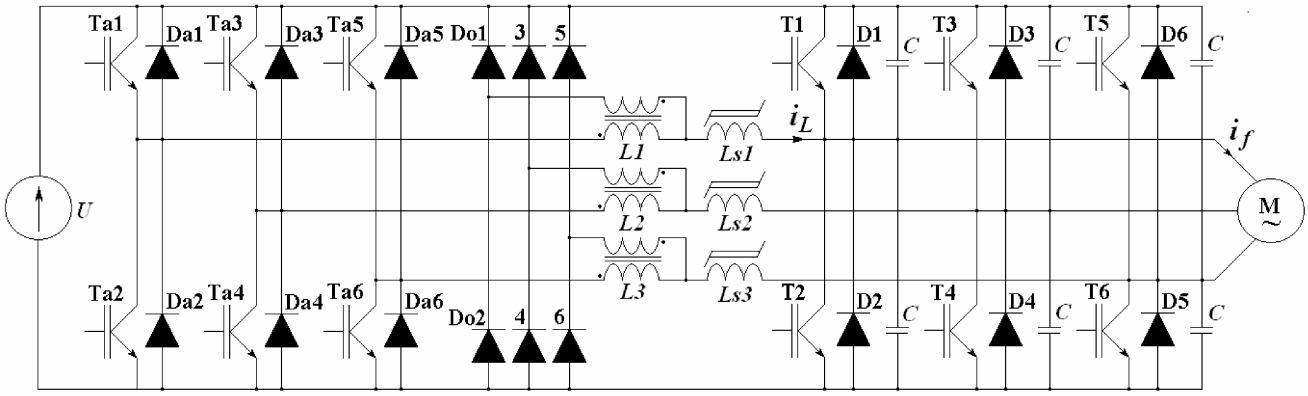

Fig. 1. Three-phase soft-switching inverter with coupled inductors

*e-mail: enesk@tu.kielce.pl

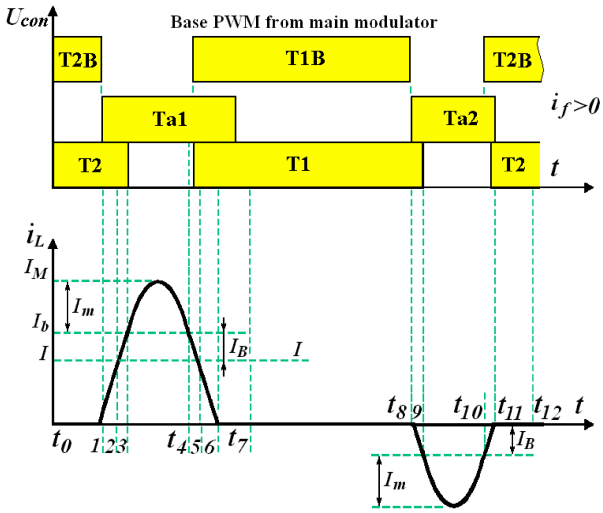

Fig. 2. Current i_L and control signals for i_f ¿0

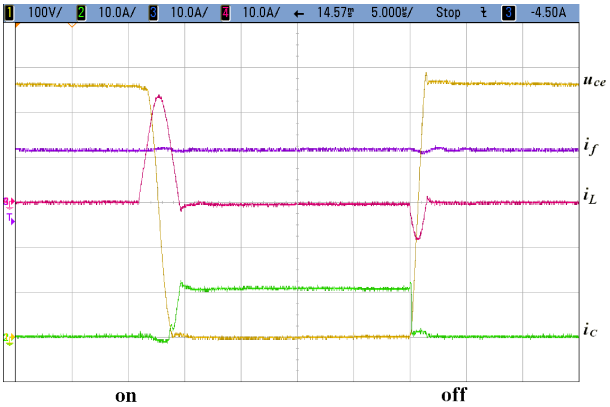

Fig. 3. Currents in one inverter leg for $i_f > 0$, standard switching, where i_L – current in the auxiliary branch, u_{ce}, i_c – collector-emitter voltage and collector current of the high voltage side main transistor.

If we assume that $i_f > 0$, then before the t_1 time the phase load current flows through diode D2. To turn on the main transistor T1 in the ZVC conditions, first the auxiliary transistor Ta1 is turned on at time t_1. The i_L current increases linearly and at time t_2 exceeds the load current $i_f = I$. The additional current I_B has to compensate the loss in the resistance of the resonant circuit. When the T2 transistor is turned off at time t_3, the resonant reloading process of the capacitors C starts. At time t_4, the upper capacitor C is completely discharged and diode D1 conducts at time period t_{45}. It allows turning on the main transistor T1 at ZVS conditions. After time t_5 the i_L current decreases linearly to zero. The inductance L_{S1} leaves the saturation state at the time t_6 and constitutes high impedance for the resonant frequency. The residual magnetizing current of the auxiliary transformer decays, flowing through diodes Da2, Do1 at time period t_{67}. If the load current is small, then to turn off the main transistor T1, the auxiliary transistor Ta2 is switched on at time t_8. The i_L current increases linearly in the opposite direction and at time t_9 reaches the $-I_B$ value. The main transistor is turned off at ZVS condition and the capacitor C with resonant inductance generates oscillations. At time t_{10} the lower capacitor C is completely discharged and diode D2 starts to conduct. During the time period t_{1112}, the diodes Da1, Do2 conduct the residual magnetizing current of the auxiliary transformer. The turn off process of the main transistor is finished. Typical turn on and turn off processes of the main transistor are shown in Fig. 3.

If the load current has sufficient value to reload the capacitor C during the dead time, the auxiliary transistors are not used. The turn off process is controlled in hard switching manner; this situation is shown in Fig. 4.

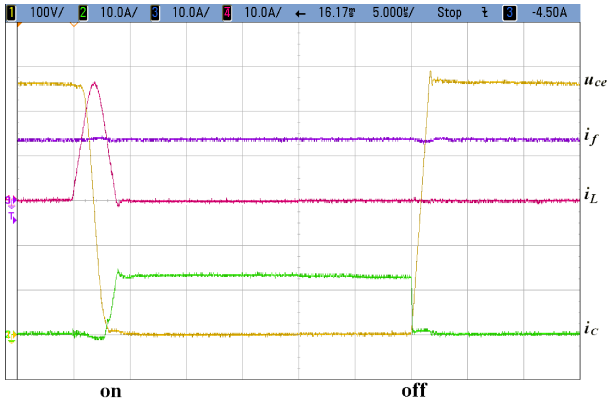

Fig. 4. Currents in one inverter leg for $i_f > 0$, turn off process without using auxiliary switches

2. Control methods

The classic control method uses constant time control signals that are adjusted according to the maximum value of the load current (equal to the nominal amplitude of the sinusoidal shape load current $I_{\max}$). In result a high amplitude resonant current appears in the auxiliary circuit. The standard value of the transformer ratio is 1:1. Theoretically the i_L current has the constant value equal to the sum of the $I_{\max}$ and the amplitude of the resonant current I_m given by

$$i_L = I_{\max} + I_m = I_{\max} + \frac{U}{2Z}, \tag{1}$$

where Z – characteristic impedance of the resonant circuit, $I_{\max}$ – amplitude of the load current $i_f = I_{\max} \sin \omega t$.

The experimental results shown in Fig. 5 display that value of the current i_L slightly changes together with instantaneous value of the load current. This phenomenon is the result of the change of the main diodes reverse recovery time t_{rr}. The t_{rr} increases with the diode forward current, the time t_3 grows up and the current i_L becomes greater.

The advanced control of the soft-switching inverter with coupled inductors ought to regulate the width of the control signals dependently on the instantaneous value of the load current. This control is called variable-time and the current i_L is given by

$$i_L = i_f + I_m. \tag{2}$$

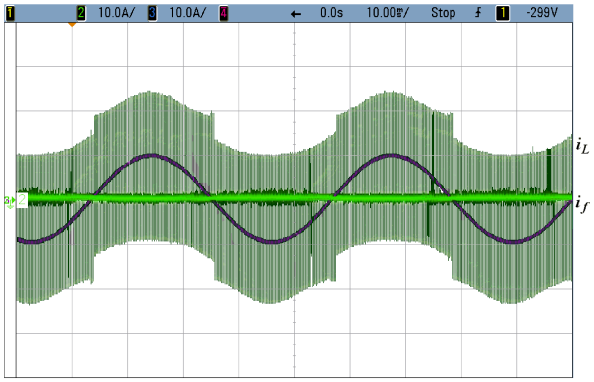

Fig. 5. Current in the auxiliary branch i_L and load current i_f, classic control

Figure 6 shows that the current i_L follows up the load current i_f. Thanks to the reduction of the i_L current amplitude, the conduction loss in the auxiliary circuit decreases. In regions where the load current is high, the turn off process of the main transistor is performed without auxiliary circuit, Fig. 7. Thanks to that an additional loss limitation is obtained.

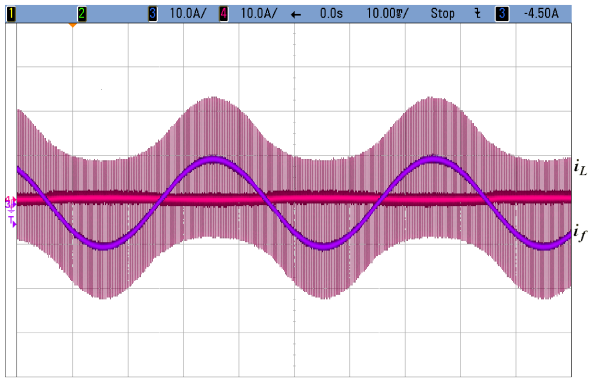

Fig. 6. Current in the auxiliary branch i_L and load current i_f, variable-time control

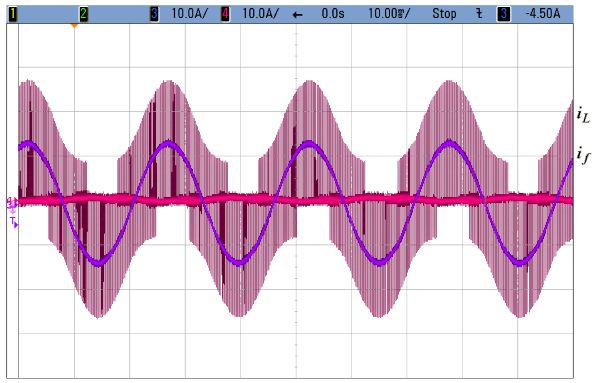

Fig. 7. Turn off process without auxiliary circuit participation at high load current regions, variable-time control

3. Review of the resonant tank elements design methods

Design of the resonant tank elements has strong influence on efficiency. For the soft-switching inverter with coupled inductors the same design procedure as for ARCP inverter is used. The most popular procedure described in [5] strongly recommends using as high resonant capacity as possible. It helps to decrease the turn off loss, but as it was shown in [6], the amplitude of the resonant current grows up and the loss in the resultant resistance of the resonant circuit increases much faster (in square of i_L). In result, the total loss remains greater. The design procedure based on energy minimisation in the resonant circuit is shown in [7]. Despite of far simplifications, obtained solutions are very complicated and can be hardly used in practice. In [6] a new design method, also based on energy minimisation, was described, but derived Eqs. (3), (4) are very clear and easy to use.

$$L = \frac{aUT_R}{4\pi I}, \tag{3}$$

$$C_R = \frac{IT_R}{a\pi U}, \tag{4}$$

where $a = 1 + \sqrt{\pi/Q}$ – coefficient, Q – quality factor, U – DC link nominal voltage, I – nominal load current, T_R – resonant period.

The resonant inductance L in the Eq. (4) contains the resultant leakage inductance L_Z of the auxiliary transformer given by (5).

$$L_Z = L_p + L_s k^2, \tag{5}$$

where L_p – leakage inductance of the primary windings, L_s – leakage inductance of the secondary windings, k – transformer turns ratio.

4. Experimental results

To verify the control method influence on the loss level, the 6 kW experimental inverter with coupled inductors shown in Fig. 8 was build.

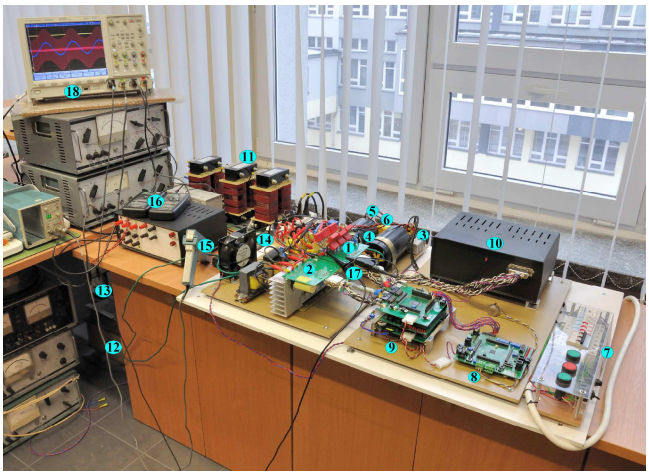

Fig. 8. Research station of the soft-switching inverter with coupled inductors

The main elements of the station are: 1. Main inverter, 2. Auxiliary switches, 3. Three-phase diode bridge rectifier, 4. Capacitor set in DC link, 5. Auxiliary two-phase diode rectifier, 6. Pre-load resistor – R, 7. Contactor set S1, S2, 8. Superior modulator system SVM, 9. Control unit of the ARCP

inverter, 10. Voltage supply with 12 isolated output voltages, 11. Load inductors L_f, 12. DC-link indictor L_{dc}, 13. Load resistors R_f, 14. Auxiliary transformers, 15. DC-link current probe, Tektronix A6303, 16. Rogowski stripe for the resonant current measure, CWT15B, 17. DC-link voltage probe, Tektronix P5120, 18. Oscilloscope Agilent MSO7034A.

In Fig. 9 the block diagram of the research station is shown.

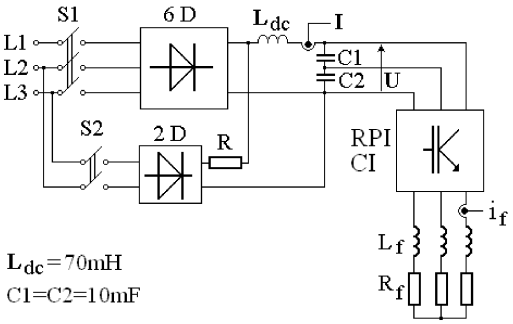

Fig. 9. Block diagram of the research station

The resonant-pole soft-switched inverter with coupled inductors (RPICI) is fed through six diode bridge (6D) from three-phase power net. In each phase, the load consist of serially connected resistors R_f (13.38 Ω) and inductances L_f (25 mH). The input power is described by Eq. (6) and the output power by (7).

$$P_{IN} = I_{AV} U_{AV}, \tag{6}$$

$$P_O = 3 I_{fRMS}^2 R_f. \tag{7}$$

Above equations make it possible to calculate the inverter efficiency (8)

$$\eta = \frac{P_O}{P_{IN}}. \tag{8}$$

The inverter was tested at hard switching mode and soft switching mode with classic and variable time control. The total power $P_T = P_{IN} - P_O$ related with loss for different carrier frequency: $f_s = 5$ kHz and $f_s = 10$ kHz, respectively, are shown in Figs. 10 and 11.

Figures 12 and 13 show the efficiency of the inverter.

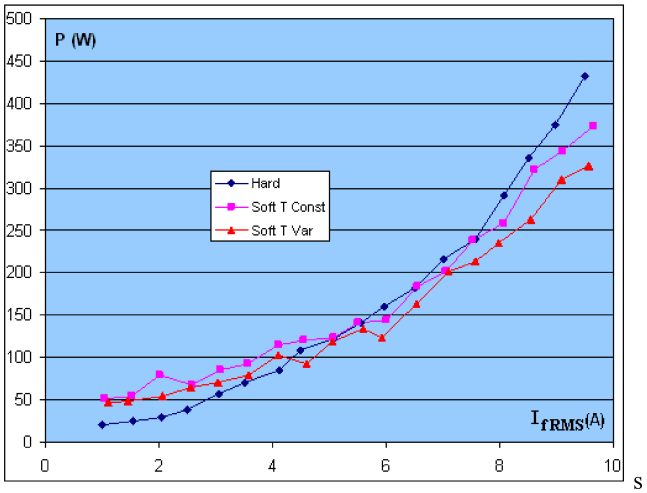

Fig. 10. Power P_T versus phase load current I_{fRMS} for $f_s = 5$ kHz

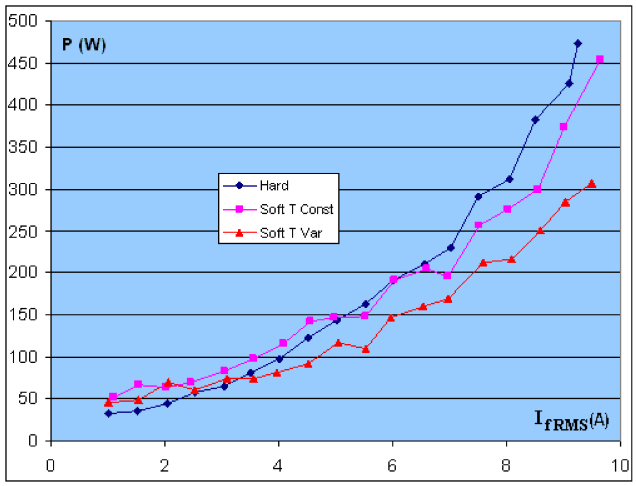

Fig. 11. Power P_T versus phase load current I_{fRMS} for $f_s = 10$ kHz

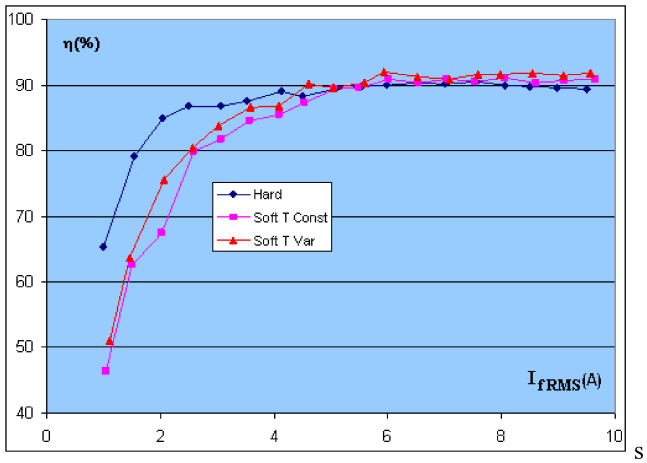

Fig. 12. Efficiency η versus phase load current I_{fRMS} for $f_s = 5$ kHz

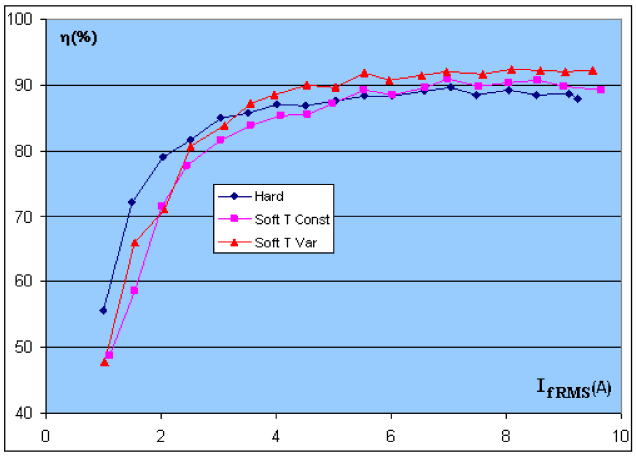

Fig. 13. Efficiency η versus phase load current I_{fRMS} for $f_s = 10$ kHz

To confirm the relationship between efficiency characteristics, the temperature of the radiator was measured. Results obtained with Fluke 52 temperature meter were placed in the Table 1.

Table 1
Measured values

Commutation type		Hard sw.	Soft – classic	Soft – variable time
Input voltage U_{AV}	V	547.0	542.0	541.0
Input current I_{AV}	A	5.1	5.1	5.1
Phase load current I_{fRMS}	A	8.0	8.0	8.0
frequency f	Hz	32.1	31.0	31.4
Carrier frequency f_s	kHz	10	10	10
Initial temperature T_P	°C	17.0	17.0	17.0
End temperature T_K	°C	36.1	35.1	34.6

The temperature distribution (for $f_s = 10$ kHz) was registered by means of the NEC G120 thermo vision recorder and shown in: Fig. 14 – hard switching, Fig. 15 – soft switching classic control and Fig. 16 – soft switching variable-time control.

Fig. 14. Temperature distribution of the radiator, hard switching

Fig. 15. Temperature distribution of the radiator, soft switching classic control

Fig. 16. Temperature distribution of the radiator, soft switching variable-time control

5. Conclusions

Introducing an advanced variable-time control, the significant loss reduction in the analyzed inverter can be obtained. It can be seen from Fig. 13, that the inverter efficiency for load current $I_{fRMS} = 8$ A increases about 2% for the variable-time control in comparison with the two other control methods. Also the temperature of the radiator shown in the Table 1 is 1.5°C lower than in hard switching control case and 0.5°C lower than in classic control mode. During measurement the fan shown in Fig. 8 was turned on. The temperature distribution shown in Figs. 14–16 inclines to state that both the temperature in the centre of the radiator (sign by X) and maximum temperature (marked by M) is significantly lower for soft-switching than for had switching mode. However, the variable-time control guarantees the lowest temperature of the radiator. The values of the resonant tank elements for $U = 538$ V, $I_{fRMS} = 10$ A, $T_R = 4.4$ μs, $x = a = 1.125$ calculated from (3), (4) are $L = 15$ μH, $C_R = 32.7$ nF. Measured resultant leakage inductance of the auxiliary transformer is equal to $L_Z = 8.6$ μH. It means that to meet minimum energy oscillation in the resonant circuit criterion, the additional inductance $L_d = L - L_Z = 6.4$ μH has to be connected serially with L_S. Generally, in this kind of inverter only the resultant leakage inductance L_Z is used as a resonant inductance L. It unnecessarily increases an amplitude of the resonant current, so the total loss becomes greater. Therefore, this approach has to be changed. An efficiency improvement has several benefits: increases range of the electric car, reduces size of the radiator, enables to use a greater carrier frequency.

REFERENCES

[1] W. Dong, J. Choi, Y. Li, H. Yu, J. Lai, D. Boroyevich, and F.C. Lee, "Efficiency considerations of load side soft-switching inverters for electric vehicle applications", *Proc. IEEE-APEC* 1, 1049–1056 (2000).

[2] S. Karyś, "Influence of the control method on power losses in voltage inverter with soft switching of ZVS type and with coupled inductors", *Mesurements, Automatics and Control* 9, 774–758 (2009), (in Polish).

[3] I. Barbi and D.C. Martins, "A true PWM zero-voltage switching pole with very low additional RMS current stress", *Proc. IEEE-PESC* 1, 261–267 (1991).

[4] S.C. Frame, D. Katsis, D.H. Lee, D. Boroyevich, and F.C. Lee, "A three-phase zero-voltage-commutation inverter with inductor feedback", *Proc. IEEE-PESC* 1, 4708–4716 (1997).

[5] W. Dong, J. Choi, F.C. Lee, D. Boroyevich, and J. Lai, "Comprehensive evaluation of auxiliary resonant comutated pole inverter for electric vehicle applications", *Proc. IEEE-PESC* 1, 625–630 (2001).

[6] S. Karyś, "Selection of resonant circuit elements for the AR-CP inverter", *Proc. IEEE-10th Int. Conf. on Electrical Power Quality and Utilisation* 1, 1–6 (2009).

[7] J. Dawidziuk, *Analysis of Power Losses in Polar Inverters of Voltage*, Publishing House of Białystok University of Technology, Białystok, 2002.